Acta Pharmaceutica Sinica B 2022;12(3):1254–1270

Chinese Pharmaceutical Association
Institute of Materia Medica, Chinese Academy of Medical Sciences

Acta Pharmaceutica Sinica B

www.elsevier.com/locate/apsb
www.sciencedirect.com

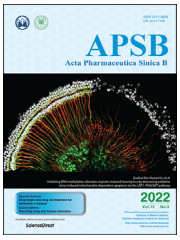

ORIGINAL ARTICLE

Peroxidase from foxtail millet bran exerts anti-colorectal cancer activity *via* targeting cell-surface GRP78 to inactivate STAT3 pathway

Shuhua Shan[a,†], Jinping Niu[a,†], Ruopeng Yin[a], Jiangying Shi[a], Lizhen Zhang[b], Caihong Wu[a], Hanqing Li[b], Zhuoyu Li[a,b,*]

[a]*Institute of Biotechnology, Key Laboratory of Chemical Biology and Molecular Engineering of National Ministry of Education, Shanxi University, Taiyuan 030006, China*
[b]*School of Life Science, Shanxi University, Taiyuan 030006, China*

Received 10 June 2021; received in revised form 31 August 2021; accepted 1 September 2021

KEY WORDS

Foxtail millet bran;
FMBP;
csGRP78;
STAT3;
ROS;
Colorectal cancer

Abstract Molecular targeted therapy has become an emerging promising strategy in cancer treatment, and screening the agents targeting at cancer cell specific targets is very desirable for cancer treatment. Our previous study firstly found that a secretory peroxidase of class III derived from foxtail millet bran (FMBP) exhibited excellent targeting anti-colorectal cancer (CRC) activity *in vivo* and *in vitro*, whereas its underlying target remains unclear. The highlight of present study focuses on the finding that cell surface glucose-regulated protein 78 (csGRP78) abnormally located on CRC is positively correlated with the anti-CRC effects of FMBP, indicating it serves as a potential target of FMBP against CRC. Further, we demonstrated that the combination of FMBP with the nucleotide binding domain (NBD) of csGRP78 interfered with the downstream activation of signal transducer and activator of transcription 3 (STAT3) in CRC cells, thus promoting the intracellular accumulation of reactive oxygen species (ROS) and cell grown inhibition. These phenomena were further confirmed in nude mice tumor model. Collectively, our study highlights csGRP78 acts as an underlying target of FMBP against CRC, uncovering the clinical potential of FMBP as a targeted agent for CRC in the future.

Abbreviations: csGRP78, cell surface glucose-regulated protein 78; CDKs, cyclin-dependent kinases; CRC, colorectal cancer; CETSA, cellular thermal shift assay; Co-IP, co-immunoprecipitation; CAC, colitis-associated carcinogenesis; DCFH-DA, dichloro-dihydro-fluorescein diacetate; ER, endoplasmic reticulum; EGFR, epidermal growth factor receptor; FMBP, peroxidase derived from foxtail millet bran; FDA, U.S. Food and Drug Administration; GRP78, glucose-regulated protein 78; H&E, hematoxylin & eosin; ISM, isthmin; MPs, membrane proteins; NBD, the nucleotide binding domain of csGRP78; PD-1, programmed death-1; ROS, reactive oxygen species; rGRP78, recombinant GRP78; STAT3, signal transducer and activator of transcription 3; SPF, specific pathogen free; SBD, substrate-binding domain of csGRP78; TRAIL, tumor necrosis factor-related apoptosis-inducing ligand.

*Corresponding author. Tel./fax: +86 351 7018268.
E-mail address: lzy@sxu.edu.cn (Zhuoyu Li).
[†]These authors made equal contributions to this work.

Peer review under responsibility of Chinese Pharmaceutical Association and Institute of Materia Medica, Chinese Academy of Medical Sciences

https://doi.org/10.1016/j.apsb.2021.10.004

1. Introduction

Colorectal cancer (CRC) ranks the world's second most deadly cancer with almost 9.6 million deaths annually[1]. Currently, CRC is commonly treated by tumor resection, as well as chemotherapy and radiotherapy, which have been proven to be limited due to their non-cancer cell specific mode of action, resulting in insufficient drug concentrations in tumors, severe adverse effects and the appearance of drug-resistant tumor cells[2]. Emerging evidence suggests that the molecular targeted agents with high specificity and less toxicity have been demonstrated promising outcomes in cancer treatment[3], mainly including small molecules, monoclonal antibodies, and immunotherapeutic cancer vaccines. Small molecule inhibitors that have been approved by the U.S. Food and Drug Administration (FDA), such as ribociclib, gefitinib and rucaparib, can target cyclin-dependent kinases (CDKs), epidermal growth factor receptor (EGFR), and poly ADP ribose polymerase (PARP), respectively, to intervene cell-cycle checkpoint, restrict cancer cell growth, and trigger cell apoptosis, leading to the blockage of cancer progression[4−6]. However, monoclonal antibodies (mAbs) specifically target antigens or membrane-bound proteins to directly exert their anti-tumor effect by interrupting the interactions between receptors and ligands. For example, nivolumab, a fully human immunoglobulin G4 PD-1 immune checkpoint inhibitor antibody, reverses immune suppression, releases T cell activation and promotes antitumor immunity *via* selectively blocking PD-1[7]. These studies indicate that the finding of tumor specific targets plays an important role in the development of antitumor targeted drugs. Therefore, screening novel specific targets for tumor targeted therapy is very meaningful.

Glucose-regulated protein (GRP78)/BIP is a major chaperone in the endoplasmic reticulum (ER) of normal organs, while in tumor cells, except for locating in ER, GRP78 is discovered in other cellular locations including the cell surface, cytosol, mitochondria, and the nucleus[8]. Importantly, GRP78 abnormally locates on surface of many cancer cells, such as lung, breast, colon, and liver cancers, but rare expression in normal cells and *in vivo* offers the opportunity for tumor-specific therapy and drug delivery without harming the normal organs. Especially, accumulation of evidence has demonstrated that csGRP78 promotes the aggressiveness of cancer disease, and has been discovered its prospect as a target of anticancer drug[9,10]. As a cell surface signaling receptor, multiple ligands of csGRP78 trigger various downstream cell signaling pathways to regulate proliferation, survival, and apoptosis of cancer[11]. Arap et al.[12] developed two targeted phage peptides with predicted binding motifs for GRP78, and found that the peptides were able to specifically bind csGRP78 to suppress tumor growth. MAb159, a high affinity csGRP78 specific mouse monoclonal IgG antibody, induced the intrinsic and extrinsic apoptosis pathway in CRC by triggering endocytosis and degradation of csGRP78[13]. Furthermore, csGRP78 can also specifically bind to Kringle5[3,14], Par-4[15], and purified GBP-SubA[16], which further drives apoptosis of cancer cells. Our previous studies revealed that the expression of csGRP78 on CRC membrane was positively correlated with its degree of malignancy[17], and we found that a reconstructed protein containing GRP78 binding peptide and mung bean trypsin inhibitor displayed significant anti-CRC effects both *in vitro* and *in vivo*[18], indicating csGRP78 serves as a potential target for CRC treatment.

In our previous studies, a novel 35 kDa secretory peroxidase of class III (FMBP) extracted from foxtail millet bran displayed prominent anti-CRC effects *in vitro* and *in vivo*[19−21], including restraining the proliferation, inducing cell apoptosis and inhibiting cell migration in CRC cells. Importantly, it had no significant effect in normal colonic epithelial cells, suggesting its specificity for CRC cells. However, the molecular target of FMBP against CRC remains unclear. According to our present findings, there is a direct interaction between FMBP and csGRP78, and interestingly, the expression level of csGRP78 in CRC cell surface is positively correlated with the anti-CRC effect of FMBP. Further, FMBP suppresses the activation of its downstream signal transducer and activator of transcription 3 (STAT3) by selectively binding to csGRP78 in CRC cells, followed by the intracellular accumulation of ROS, finally resulting in the blockade of CRC development. These results reveal that csGRP78 serves as a potential target of FMBP against CRC. Importantly, FMBP has the clinical potential to be developed as a targeted agent for CRC.

2. Materials and methods

2.1. Chemical reagents and antibodies

Foxtail millet bran was supplied from Tian-xia-gu Co., Ltd. (Taiyuan, China). SP Sepharose XL ion exchange resin was purchased from GE Healthcare (Uppsala, Sweden). RPMI-1640 medium, F-12 medium, DMEM medium and fetal bovine serum (FBS) were obtained from GIBCO (Grand Island, NY, USA). Penicillin−Streptomycin−Gentamycin Mixed Solution, polybrene and puromycin were obtained from Solarbio (Beijing Solarbio Science & Technology Co., Ltd.). BCA protein assay kit, reactive oxygen species assay kit and calcium phosphate cell transfection kit were provided by Beyotime Institute of Biotechnology (Haimen, China). 3-(4,5-Dimethyl-2-thiazolyl)-2,5-diphenyl-2*H*-tetrazolium bromide (MTT) and dimethyl sulfoxide (DMSO) were obtained from Sigma (St. Louis, MO, USA). Annexin V-APC/7-AAD Apoptosis Detection Kit and Membrane, Nuclear and Cytoplasmic Protein Extraction Kit were obtained from KeyGEN BioTECH Co., Ltd. (Nanjing, China). Long-arm Biotin Labeling Kit was obtained from Elabscience Biotechnology Co., Ltd. (Wuhan, China). TRAIL was purchased from R&D Systems (Abingdon, UK). Avidin-agarose beads were purchased from Biomag Biotechnology Co., Ltd. (Wuxi, China). Garcinone D was purchased from Shanghai Yuanye Bio-Technology Co., Ltd. (Shanghai, China). The antibody for GRP78 and Protein A/G PLUS-Agarose were obtained from SantaCruz Biotechnology, Inc.

(Santa Cruz, CA). Antibody for STAT3 was purchased from Sangon Biotech Co., Ltd. (Shanghai, China). Antibody for p-STAT3 (phosphor Y705) was purchased from Abcam Trading Co., Ltd. (Shanghai, China). Antibody for GAPDH was purchased from Boster Biological Technology Co., Ltd. Polyfect® was obtained from Qiagen (Hilden, Germany).

2.2. Cell culture

Human colon carcinoma cell lines DLD1, HCT-116, HT-29 and LS174-T were purchased by the Cell Bank of Type Culture Collection of the Chinese Academy of Sciences (CAS, Shanghai, China), and human colon epithelial cell line FHC was purchased from the American Type Culture Collection (ATCC, USA). DLD1 and HT-29 cells were grown in RPMI-1640 medium supplemented with 10% (*v*/*v*) heat-inactivated fetal calf serum, 2 mmol/L glutamine, 100 units/mL penicillin, and 100 μg/mL streptomycin (Sigma; St. Louis, MO, USA) at 37 °C in a 5% CO_2 humidified atmosphere. HCT-116 and FHC cells were grown in F12 medium. LS174-T cells were grown in DMEM medium.

2.3. Preparation of FMBP and its biotinylation

Purification of FMBP was performed according to our previous described method[19]. Foxtail millet bran was soaked in deionized 0.02 mol/L Tris-HCl buffer for 24 h, and then the supernatant was precipitated with 80% saturated ammonium sulfate at 4 °C for 30 min, followed by purification with SP cation-exchange column. The eluted fraction of 100 mmol/L NaCl was collected and incubated for 20 min at 80 °C and showed a single band on SDS-PAGE, named FMBP.

FMBP was treated with Long-arm Biotin Labeling Kit (Elabscience Biotechnology Co., Ltd.) according to the manufacturer's instructions, and then the Bio-FMBP was obtained. Briefly, 1 mg of FMBP was dissolved in 0.5 mL label buffer and added into ultrafiltration tube. After centrifuged 12,000 × *g* for 10 min, appropriate NH_2-Reactive Biotin and labeling buffer were added to the filtration tube with gently blowing blending. The mixture was incubated in darkness at 37 °C for 30 min, followed by centrifugation at 12,000 × *g* for 10 min, and then washed twice with labeling buffer. The ultrafiltration tube was inverted in a new EP tube and centrifugated at 6000 × *g* for 10 min. The biotin-labeled FMBP solution was collected and kept at 4 °C.

2.4. Cell survival assay

Cell survival assay was performed using MTT method. Briefly, DLD1 and HCT-116 cells pre-incubated with 4 μg/mL anti-GRP78 antibody for 1 h, LS174-T cells pre-treated with 100 ng/mL TRAIL for 180 or 240 min, LS174-T cells transiently transfected with different plasmids (GFP, GFP-GRP78, or GFP-GRP78-N500) were treated with 3 μmol/L FMBP for 48 h, respectively. Next, culture supernatants were removed, followed by incubation for 4 h at 37 °C in darkness with medium containing 5 mg/mL MTT. Then, the medium was removed and 150 μL dimethyl sulfoxide (DMSO) was added. The absorbance at 570 nm was detected and the data were expressed as the mean percentage of absorbance in treated *vs*. control. The value of the control was set at 100%. Cell survival rate was calculated with Eq. (1):

$$\text{Cell survival rate (\%)} = OD_{570}\,(\text{treated})\,/OD_{570}\,(\text{control}) \times 100 \quad (1)$$

2.5. Colony-formation assay

Colony-formation assay was carried out as our previously described with some modifications[22]. DLD1 and HCT-116 cells were pre-treated with anti-GRP78 antibody for 1 h, followed by treatment with 3 μmol/L of FMBP for 5 days. Cell colonies were fixed for 20 min with 6% glutaraldehyde, and then stained with 0.1% crystal violet. Cell colony-formation ability was observed by stereoscopic microscope. Finally, these cells stained by crystal violet was dissolved with 150 μL of 1% SDS, and the absorbance at 570 nm was detected.

2.6. Identification of target protein of FMBP

Identification of target protein of FMBP was based on pull-down technology coupled with MALDI-TOF/TOF analysis. Bio-FMBP or PBS was incubated for 2 h at 4 °C with Avidin-agarose beads. Then, immobilized beads were washed for 3 times with PBS and kept at 4 °C before use. DLD1 cells were seeded into 100 mm culture dish at a density of 1×10^6 cells and grown in a humidified incubator with 5% CO_2 at 37 °C for 24 h. Cells were collected and the membrane proteins (MPs) were extracted using a commercial kit. MPs were extracted according to the manufacturer's instructions, after which MPs were divided into two aliquots: one was incubated with Bio-FMBP binding Avidin-agarose beads overnight at 4 °C, and the other was used as negative control incubated with Biotin binding Avidin-agarose beads in the same way. The precipitate was mixed with SDS-PAGE loading buffer and boiled for 10 min. The samples were loaded and separated on 10% SDS-polyacrylamide gel (PAGE), followed by silver staining (Beyotime, China) according to the manufacturer's instructions. Then, the different band was cut from SDS-PAGE and sent to Shanghai Applied Protein Technology Co., Ltd. (China) for protein identification by matrix-assisted laser desorption/ionization time-of-flight/time-of-flight (MALDI-TOF/TOF, Applied Biosystems, USA), followed by analysis of Uniprot Database.

2.7. Biolayer interferometry assay

The binding affinity between FMBP and GRP78 was determined by biolayer interferometry technology using the OctetRED system (ForteBio). Purified FMBP was biotinylated by Long-arm Biotin Labeling Kit (Elabscience Biotechnology Co., Ltd.) following the manufacturer's protocol. Bio-FMBP (2 mg/mL) was then incubated with super-streptavidin biosensors in binding buffer (20 mmol/L HEPES pH 7.4, 150 mmol/L NaCl) and washed three times in binding buffer. Recombinant GRP78 was serially diluted by binding buffer, and the association/dissociation of FMBP:GRP78 was monitored by OctetRED for 10 min at 25 °C. Data were analyzed using Octet Data Analysis Software 7.0 (ForteBio).

2.8. Immunofluorescence assay

Immunofluorescence assay was performed according to previous described method with some modifications[23]. HT29, DLD1, and HCT-116 cells were seeded into 24-well slides overnight, followed by treatment with 3 μmol/L Bio-FMBP for 4 h. After washing with PBS for two times, these cells were incubated with a final concentration of 1.5 mmol/L cross-linker DTSSP (Thermo Scientific) solution for 30 min at room temperature, and crosslinking reaction was stopped after 15 min by 20 mmol/L Tris-HCl buffer

reaction (PH 7.5), respectively. Cells were fixed in 4% paraformaldehyde in PBS for 30 min, and then blocked in 10% goat serum for 1 h, followed by incubation with anti-GRP78 primary antibody and the corresponding secondary antibody. Nuclei was stained using ProLong® Gold Antifade Mountant with DAPI (Thermo Scientific). After washing with PBS for three times, the slides were mounted in gelvatol for confocal immunofluorescence analysis.

2.9. Cellular thermal shift assay (CETSA)

CETSA was performed according to previous described method with some modifications[24]. DLD1 cells were seeded into 60 mm culture dish at a density of 1×10^6 cells and grown in a humidified incubator with 5% CO_2 at 37 °C overnight. Cells were collected and the membrane proteins (MPs) were extracted according to the method described in Section 2.5, and then the MPs were divided into two equal parts, with one incubated with FMBP (20 μmol/L) and the other as control (PBS). After incubation for 10 min at room temperature, the mixture was heated individually for 3 min at different temperatures (45−80 °C) followed by cooling for 3 min at room temperature. Then, the levels of csGRP78 were analyzed by Western blot assay.

2.10. Competitive inhibition assay

DLD1 cells were collected and the membrane proteins (MPs) were extracted according to the manufacturer's instructions. Next, the MPs were incubated for 4 h with different concentration of FMBP (0, 20, 40, or 60 μmol/L), respectively, followed by co-incubation overnight with Bio-FMBP binding Avidin-agarose beads. The beads were mixed with SDS-PAGE loading buffer and boiled for 10 min. The samples were loaded and separated on 10% SDS-PAGE, followed by Western blot analysis.

2.11. Cell surface translocation of GRP78 induced by TRAIL

Cell surface proteins were analyzed using flow cytometry as previously described[25]. To analyze the expression level of csGRP78 on LS174-T cell membrane, LS174-T cells were seeded in 60 mm cell culture dish, and then treated with TRAIL for 180 or 240 min. The cells were collected after being digested with trypsin. After washed with pre-cooled PBS for three times, the cells were incubated with anti-GRP78 primary antibody for 2 h at room temperature, followed by incubation for 30 min at 4 °C in the dark with appropriate volume of FITC-conjugated secondary antibody. As controls, cells were incubated with the secondary IgG alone. After wrapped in foil to avoid light, the cells were added into flow tube for analysis on EPICS XL flow cytometry.

2.12. Measurement of reactive oxygen species (ROS) generation

The intracellular level of ROS was analyzed by flow cytometry as described previously[22]. Briefly, DLD1 and HCT-116 cells or LS174-T cells were seeded in 60 mm cell culture dish and cultured overnight at 37 °C with 5% CO_2. DLD1 and HCT-116 cells were pretreated with 4 μg/mL anti-GRP78 antibody for 1 h, and LS174-T cells were transfected with plasmids (GFP, GFP-GRP78 or GFP-GRP78-N500) for 24 h, after which they were treated by 3 μmol/L FMBP for 48 h, respectively. Then, the cells were washed twice with PBS and stained for 30 min with 10 μmol/L DCFH-DA at 37 °C in the dark. ROS generation was determined by formation of fluorescent dichlorofluorescein (DCF). Cells were collected and the fluorescence intensities were measured by flow cytometry.

2.13. Transient transfection assay and screening LS174-T cell line of stably overexpressed GFP-GRP78-N500

Transient transfection assay was performed with polyfect transfection reagent (Qiagen)[26]. Briefly, LS174-T cells were cultured in 6-well dish at a density of 4×10^5 cells in a 37 °C, 5% CO_2 incubator overnight. Plasmid DNA (GFP, GFP-GRP78, GFP-GRP78-N500) was first dissolved in 1/10 of the final cell culture volume of DMEM, free of serum and antibiotics. Then followed by incubation with appropriate transfection reagent for 10 min at room temperature, it was added to the cells in culture. After 6 h, the medium was changed to DMEM, supplemented with 10% FBS and antibiotics. The commercially available reagent Polyfect® was used for transfection according to the manufacturer's instructions. Parallel experimental cell lysates were collected for Western blot analysis to confirm the overexpression of plasmids in all experiments.

For lentiviral packaging, the packaging plasmid psPAX.2, the envelope plasmid pMD2.G and the plvx-AcGFP-puro vector or plvx-AcGFP-GRP78-N500-puro vector were triply transfected into HEK-293T cells. After transfection, the supernatant fraction containing lentiviral particles was harvested at 48 and 72 h, respectively. LS174-T cells were infected in the presence of 8 μg/mL polybrene. Medium containing puromycin was added every 2 or 3 days to screen the GFP-GRP78-N500 stably expressed cell lines (LS174-T/GFP-GRP78-N500 or LS174-T/GFP) until the uninfected cells were almost completely removed.

2.14. Cell apoptosis assay

Cells apoptosis ratio was detected by flow cytometry (BD Bioscience, San Jose, CA, USA). DLD1 and HCT-116 cells were pre-treated with anti-GRP78 antibody for 1 h, followed by treatment with 3 μmol/L of FMBP for 48 h, while LS174-T cells were treated according to the method described in Section 2.11. Then, cells were digested by trypsin, and washed twice with PBS, followed by stained by Annexin-V and propidium iodide (PI), while LS174-T cells transfected by different plasmids were stained with Annexin V-APC and 7-AAD. Finally, cell apoptosis ratio was detected by flow cytometry.

2.15. Western blot analysis

As mentioned above, DLD1 cells were treated as the methods described in Sections 2.9 and 2.10, while LS174-T cells were treated as the methods described in Sections 2.11 and 2.12. Cells were collected and the membrane proteins (MPs) were extracted according to the manufacturer's instructions. The equivalent amount of protein (80 μg) in each sample were separated by electrophoresis in 10% SDS-PAGE and transferred to the polyvinylidene fluoride (PVDF) membranes for probing with antibodies. After washing with Tris-buffered saline/Tween-20 buffer, membranes were blocked by 5% skimmed milk for 1 h at room temperature, followed by incubation with primary antibodies against GRP78, GFP, STAT3, p-STAT3 and the corresponding secondary antibodies. Then, bands were detected using enhanced chemiluminescence regents in a dark room.

2.16. Co-immunoprecipitation (Co-IP) assay

Co-IP assay was performed as our previously described[27]. Briefly, DLD1 cells were harvested and homogenized in radioimmunoprecipitation assay (RIPA) lysis buffer (Beyotime, China) containing a protease inhibitor cocktail. A final volume (1 mL) of whole-cell lysates (WCLs, 500 μg protein) were pre-cleared by incubation with 1.0 μg control IgG corresponding to the host species of the anti-STAT3 primary antibody together with 20 μL of Protein A/G PLUS-Agarose (Santa Cruz, CA, USA) for 2 h at 4 °C, followed by centrifugation at 500 × *g* at 4 °C for 5 min. The supernatant was subjected to immunoprecipitation by adding 2 μg of immunoprecipitation anti-STAT3/IgG antibody, and incubated overnight at 4 °C, followed by incubation with Protein A/G PLUS-Agarose for 2 h. After washing 4 times with cell lysis buffer, the beads were boiled in 2 × SDS loading buffer, and the supernatants were resolved by SDS-PAGE and subjected to Western blot analysis.

2.17. In vivo studies

BALB/c male nude mice (5-week-old) were purchased from National Institutes for Food and Drug Control and were housed in a Specific Pathogen Free (SPF) facility of China Institute for Radiation Protection under the normal laboratory conditions. All animal experiments were carried out following procedures approved by the Institutional Animal Care and Use Committee of China Institute for radiation protection. The named Institutional Review Board or Ethics Committee specifically approved this study.

LS174-$T^{GFP\text{-}GRP78\text{-}N500}$ or LS174-T^{GFP} cells (2.5×10^6) in 0.2 mL PBS were injected subcutaneously into the left oxter of each nude mouse. Solid tumors in all injected nude mice were apparent after two weeks. Next, mice were randomly divided into four groups (10 mice each group), including GFP group, GFP + FMBP group, GFP-GRP78-N500 group, and GFP-GRP78-N500+FMBP group. Mice in FMBP groups received an intraperitoneal injection administration of 100 mg FMBP/kg body weight every three days, and the control mice (GFP or GFP-GRP78-N500) were treated with PBS instead. Tumor diameters were serially measured using an electronic caliper, and tumor volumes were calculated using Eq. (2)[28]:

$$\text{Tumor volume (cm}^3\text{)} = 0.5 \text{ Tumor length (cm)} \times \text{Tumor width}^2 \text{ (cm}^2\text{)} \quad (2)$$

On the 21st day of FMBP treatment, all mice were sacrificed. Tumors were excised, weighted and fixed for further immunohistochemistry analysis.

2.18. Histopathology and immunohistochemistry assays

The main organs and tumors of all nude mice were fixed with 4% buffered formalin and embedded in paraffin. Next, these fixed organs were stained using hematoxylin and eosin (H&E) to observe histological features. Meantime, immunohistochemistry examinations for GRP78, Ki67, p-STAT3 and activated-caspase3 of sections obtained from 10% paraffin-embedded tissues were carried out as previously described[19]. Subsequently, these stained sections were visualized and photographed under inverted microscope (200 × magnification). The IHC data were quantified by Image J software.

2.19. Statistical analysis

Data were presented as means ± standard deviation (SD) calculated over three independent experiments performed in triplicate. Origin Pro 8 software was used to create the artwork. For Western blot results, protein bands were visualized using Image J gelanalyzer software. Multiple comparisons were analyzed by one-way factorial analysis of variance (ANOVA) and different letter indicates significant differences ($^*P < 0.05$). The data were statistically analyzed using Student's *t*-test by SPSS 18.0 software, with $P < 0.01$ considered highly significant differences between two groups ($^{**}P < 0.01$, $^{***}P < 0.001$).

3. Results

3.1. csGRP78 is a specific interaction protein binding with FMBP

Immunofluorescence analysis indicated that FMBP mainly located on the surface of CRC cell membrane, rather than enter cells (Supporting Information Fig. S1). Next, a biotin-tagged FMBP probe (Bio-FMBP) was used to pull down the CRC cell surface target of FMBP, and biotinylated label had no effect on the anti-CRC activity of FMBP (Supporting Information Fig. S2). Pull-down assay coupled with sliver staining showed that compared to control group, one different protein band was observed between 70 and 90 kDa in the pull-down group with Bio-FMBP beads (Fig. 1A). Next, a different band was identified as glucose regulatory protein 78 (GRP78) by MALDI TOF/TOF analysis coupled with Uniprot Database (Fig. 1B and C). Therefore, we speculate that csGRP78 may be the specific interaction protein binding with FMBP on CRC cell membrane. Subsequently, the interaction of FMBP with GRP78 *in vitro* was further confirmed by biolayer interferometry analysis using purified FMBP and recombinant GRP78 (rGRP78). As shown in Fig. 1D, FMBP bound to rGRP78, and the binding was moderately strong with a binding coefficient of 1.024×10^{-7}, which indicates that there is a direct interaction between FMBP and GRP78. Cellular thermal shift assay (CETSA) is based on the biophysical principle of ligand-induced thermal stabilization of target proteins, which prominently monitors drug binding to target proteins in cells and tissue samples[24]. The studies showed that some compounds could perturb protein function and increase the protein stability *via* forming a ligand-protein complex[29,30]. Hence, we attempted to investigate whether csGRP78 binding to FMBP could increase its stability in DLD1 cells by CETSA assay. As expected, FMBP treatment efficiently protected csGRP78 protein from temperature-dependent degradation (Fig. 1E), indicating that the stability of GRP78 in DLD1 cells was enhanced by binding to FMBP. Next, the interaction of FMBP with GRP78 *in vivo* was further verified by competitive inhibition assay. DLD1 cell membrane lysates with Bio-FMBP beads in the presence or absence of an excess amount of FMBP were incubated for competitive binding, and then Bio-FMBP beads was used to pull-down csGRP78 from DLD1 cells membrane lysate. As shown in Fig. 1F, csGRP78 was obviously pulled down by Bio-FMBP beads, which were detected by Western blotting, and an excess amount of FMBP effectively blocked the binding of GRP78 to Bio-FMBP beads. These results indicate that csGRP78 is a receptor that FMBP directly binds to CRC cell membrane.

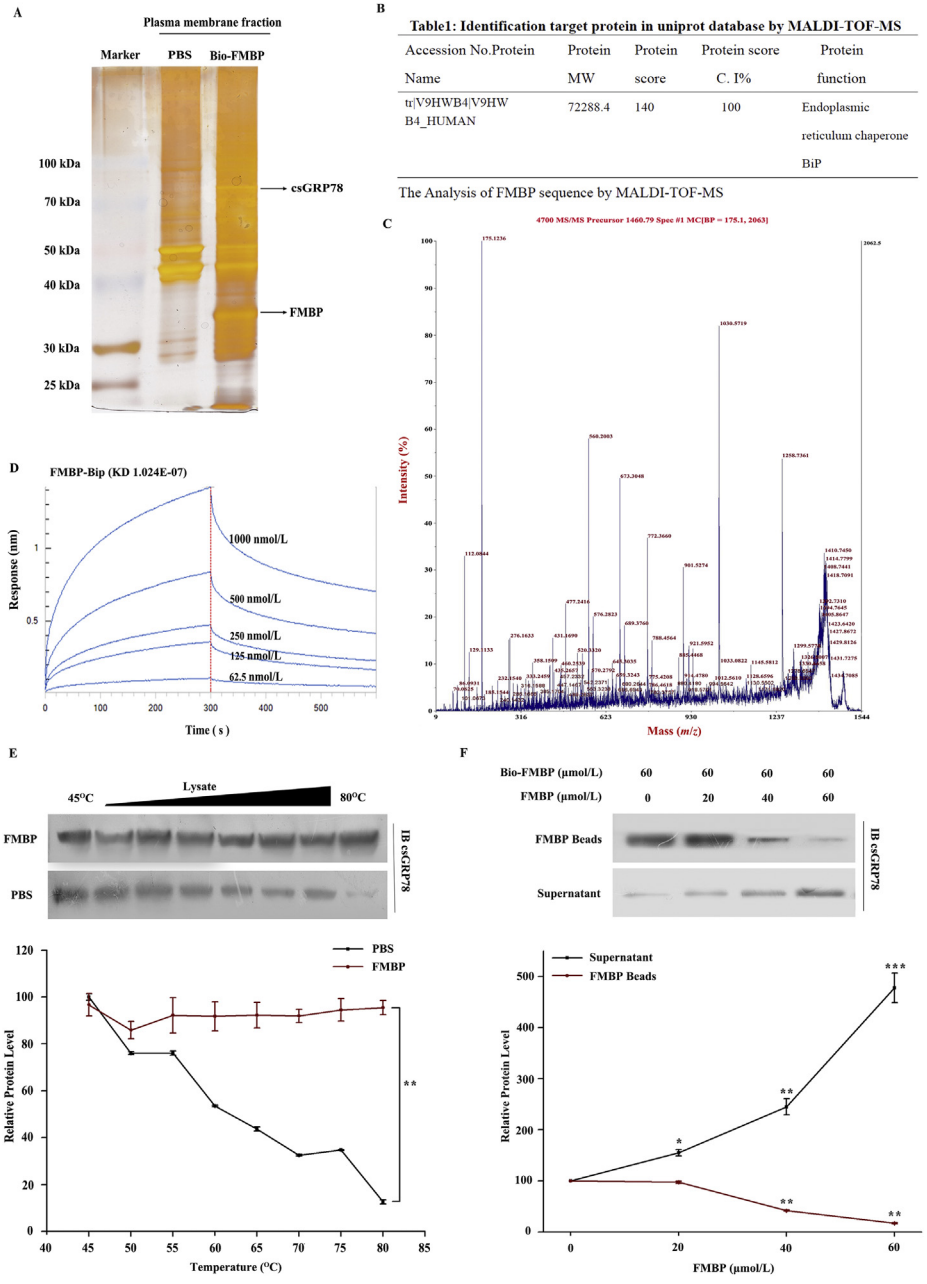

Figure 1 csGRP78 is a specific interaction protein binding with FMBP. (A) Identification of FMBP interaction proteins using pull-down technology. DLD1 cell membrane proteins were incubated with Bio-FMBP beads or control beads, and then the proteins bound to the beads were resolved by SDS/PAGE, followed by silver staining. (B) Identification target protein in uniport database by MALDI-TOF-MS. (C) The second mass spectrogram of GRP78. (D) Biolayer Interferometry analysis of interactions between GRP78 and FMBP. (E) FMBP treatment (20 μmol/L) increases the thermal stability of GRP78 in DLD1 cells was measured by the temperature-dependent cellular thermal shift assay (CETSA) ($n = 3$). (F) FMBP specifically binds to GRP78. Bio-FMBP beads were incubated with DLD1 cell membrane protein lysate in the absence or presence of FMBP for the competitive binding, and then the proteins bound to the beads were detected by Western blot assay ($n = 3$). Data are shown as the mean ± SD ($n = 3$) and analyzed by Student's *t*-test. $^{*}P < 0.05$, $^{**}P < 0.01$, $^{***}P < 0.001$.

3.2. csGRP78 expression is positively correlated with FMBP against CRC

To confirm the expression level of csGRP78 on the membrane surface of different CRC cell lines, the Western blot assay was carried out. As shown in Fig. 2A, the expression level of csGRP78 was the highest in DLD1 cells, followed by HCT-116 cells, HT29 cells, and LS174-T cells, and the lowest in FHC cells. Through the immunofluorescence co-localization assay, it was confirmed that FMBP and csGRP78 exhibited an obvious co-localization on the cell membranes of HT29, DLD1 and HCT-116 (Fig. 2B). Further, to examine whether the anti-CRC effect of FMBP is related to the expression of csGRP78, cell viability ratios of DLD1, HT29, HCT-116, LS174-T and FHC cell lines

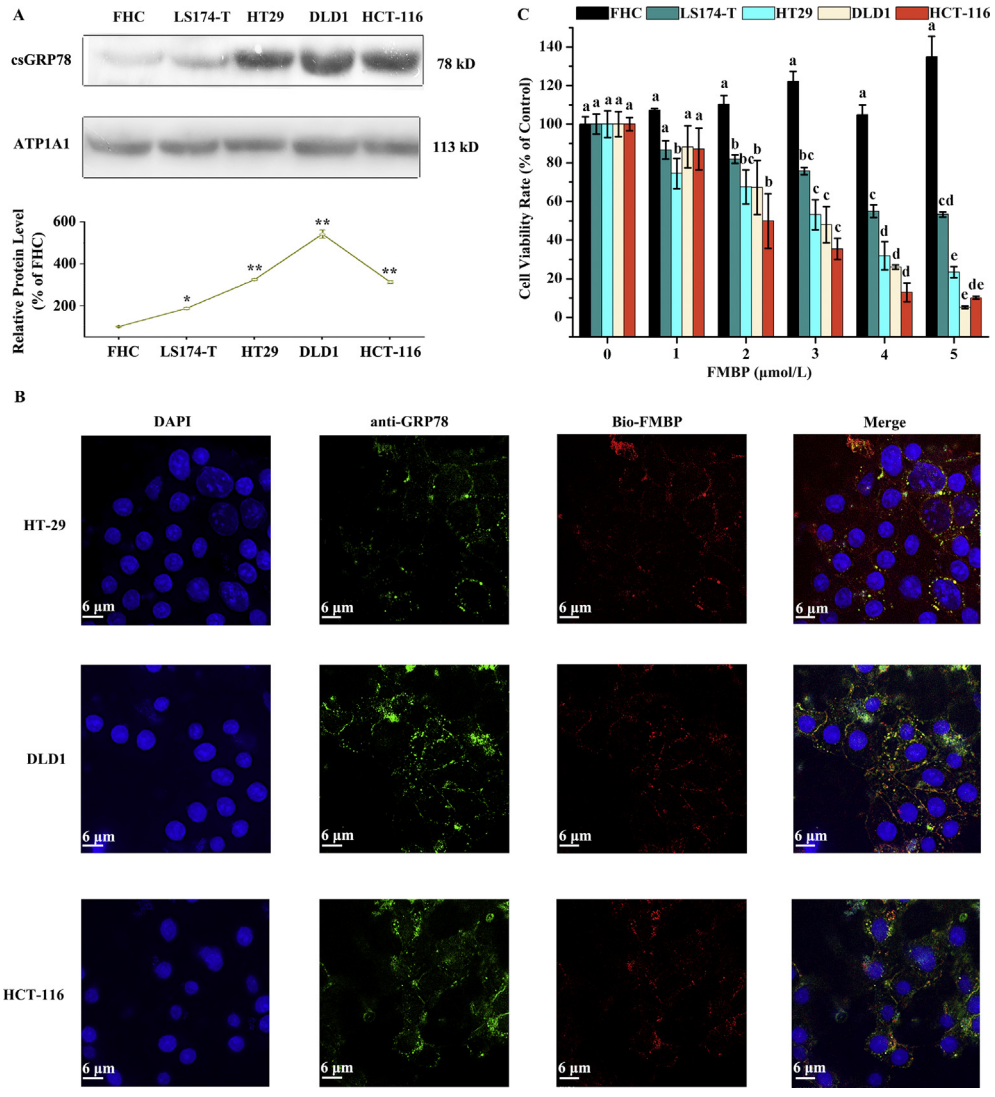

Figure 2 Anti-CRC effect of FMBP is positively correlated with the expression of csGRP78. (A) Immunoblotting of csGRP78 in normal colon epithelial cells (FHC) and in the indicated colon cancer cell lines. Data represented as the mean ± SD ($n = 3$); $^{*}P < 0.05$, $^{**}P < 0.01$. (B) Immunofluorescence of HT-29 (above), DLD1 (middle) and HCT-116 (below) cells exposed to 3 μmol/L Bio-FMBP for 4 h, and then observed under confocal microscopy. Red, FMBP; Green, csGRP78. Scale bar: 6 μm. (C) Cell viability assay of the same cell lines as in (A) treated with the indicated concentrations of FMBP for 48 h. Data represented as the mean ± SD ($n = 3$). Significant differences between the two columns were indicated by different letters, $^{*}P < 0.05$.

were measured with different concentrations of FMBP treatment by MTT assay. As presented in Fig. 2C, DLD1, HCT-116, and HT29 cells with a high expression of csGRP78 show a lower cell survival rate compared to that of LS174-T and FHC cells with a low expression of csGRP78, and the IC_{50} values were shown in Supporting Information Table S1, suggesting that the anti-CRC effect of FMBP is probably correlated positively with the expression of csGRP78 in different CRC cells.

3.3. Blocking csGRP78 of CRC almost nullified the anti-CRC activities of FMBP

As shown in Fig. 2A and Supporting Information Fig. S3, the expression level of csGRP78 was higher in DLD1 and HCT-116 cells. Therefore, to confirm the key role of csGRP78 in the anti-CRC activity of FMBP, the effects of FMBP on cell viability rate, cell clone ability, cell apoptosis and ROS level of CRC cells were measured through blocking csGRP78 with anti-GRP78 antibody. The results show that blocking csGRP78 with anti-GRP78 antibody reversed the inhibitory effect on cell proliferation and colony ability induced by FMBP (Fig. 3A–C). Moreover, as shown in Fig. 3D and E, after blocking csGRP78 with anti-GRP78 antibody, the pro-apoptotic effect of DLD1 cell induced by FMBP also showed a significant reduction. Previously, we observed that FMBP inhibited cell proliferation by producing ROS excessive accumulation in CRC cells[22]. Therefore, effect of FMBP on intracellular ROS level was measured through blocking csGRP78 with anti-GRP78 antibody by flow cytometry analysis. As expected, after blocking csGRP78, the intracellular accumulation of ROS induced by FMBP exhibited a significant decline (Fig. 3F and G). These results indicate that blocking csGRP78 with anti-GRP78 antibody in HCT-116 and DLD1 cells significantly impairs the anti-CRC activities of FMBP, suggesting that csGRP78 in CRC is crucial for the anti-CRC effects of FMBP.

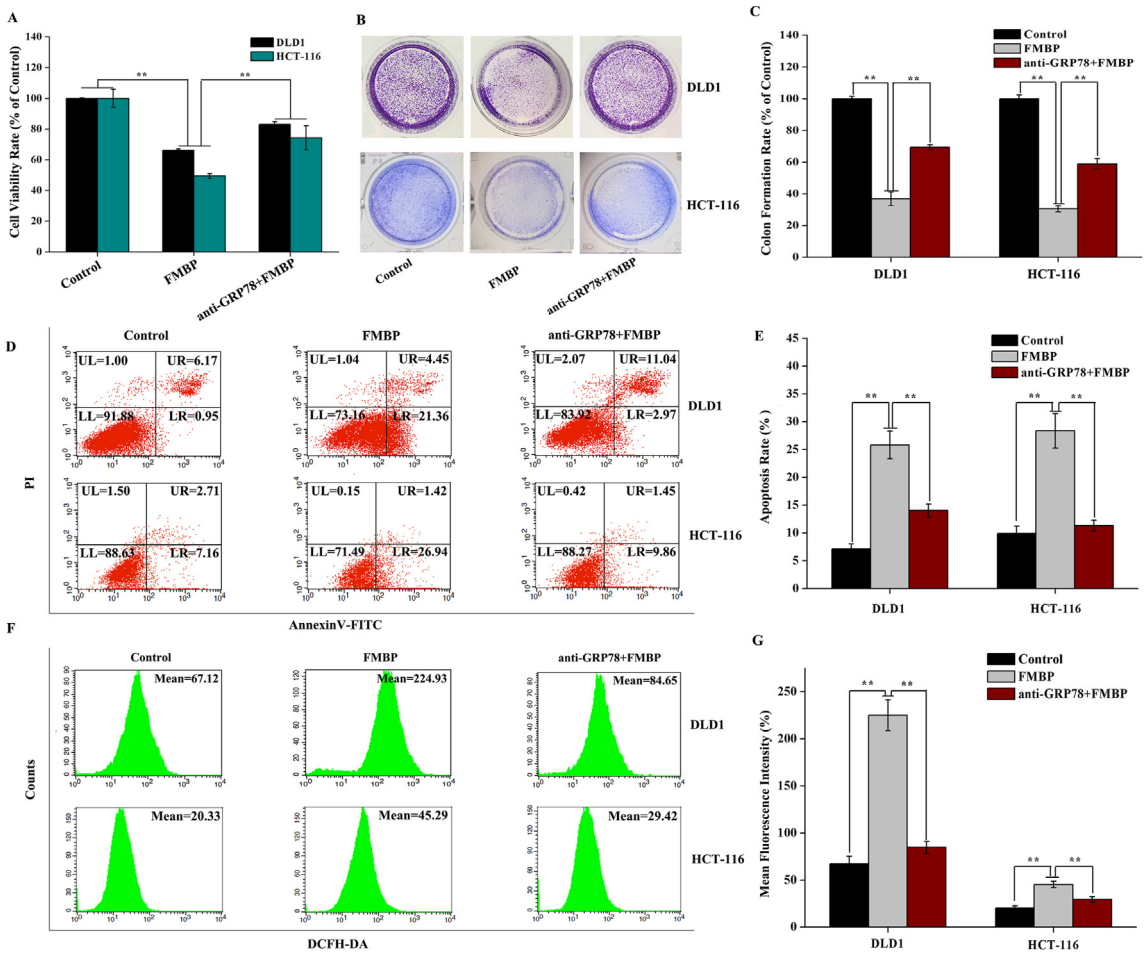

Figure 3 Reversal effects of blocking csGRP78 on FMBP against CRC. (A) Effect of blocking csGRP78 on cell survival inhibition induced by FMBP. Cell viability radios of DLD1 and HCT-116 were determined by the MTT assay. (B) and (C) Effect of blocking csGRP78 on the ability of cell colony formation induced by FMBP. Cell colony-formation ability stained by crystal violet was observed by stereoscopic microscope, and cell viability ratio was measured. (D)−(G) Effects of blocking csGRP78 on FMBP-induced cell apoptosis and ROS level were analyzed by flow cytometry. All data are shown as the mean ± SD ($n = 3$) and analyzed by Student's *t*-test. $^{**}P < 0.01$ compared with FMBP treatment.

3.4. Enhanced csGRP78 in CRC promotes the anti-CRC effect of FMBP

Tumor necrosis factor-related apoptosis-inducing ligand (TRAIL) is known to selectively induce apoptosis only in cancer cells. The study has shown that TRAIL treatment for short time intervals can induce the translocation of GRP78 from the ER to the cell surface[15]. As shown in Fig. 2A, the expression level of csGRP78 was lower in LS174-T cells. Hence, TRAIL treatment was used to improve the expression level of csGRP78 on LS174-T cell surface. As shown in Fig. 4A and B, the level of csGRP78 in LS174-T shows a drastic increase with TRAIL treatment, and its level is the highest with TRAIL treatment for 240 min. Further, the effect of TRAIL on csGRP78 expression in LS174-T cells was quantitatively analyzed by flow cytometry. FACS analysis was performed on which were not chemically fixed in order to allow the detection of csGRP78, indicating a significant increase in csGRP78 upon treatment with TRAIL (Fig. 4C and D). As expected, after pretreated with TRAIL for 180 or 240 min, the effect of FMBP on the survival of LS174-T cells was markedly decreased compared to with only FMBP treatment (Fig. 4E), and the apoptosis rate notably was significantly increased (Fig. 4F and G).

Overexpression of GRP78 can activate the re-localization of GRP78 from endoplasmic reticulum (ER) to plasma membrane[31]. To further elucidate the relationship between levels of csGRP78 in CRC cells and anti-CRC effect of FMBP, the cell survival rate, apoptosis rate, and ROS level were detected with FMBP treatment in LS174-T cells transfected by GFP-GRP78. As observed in Fig. 5A and Supporting Information Fig. S4, csGRP78 was successfully overexpressed in LS174-T cells transfected with GFP-GRP78. As expected, the sensitivity of FMBP on LS174-T cells overexpressed with GFP-GRP78 was significantly increased, characterized by the reduced cell survival rate (Fig. 5B), the enhanced cell apoptosis rate (Fig. 5C and D) and ROS accumulation level (Fig. 5E and F), compared to those of LS174-T cells transfected with GFP. These results indicate that the sensitivity of FMBP to CRC cells is mainly attributed to the expression level of csGRP78 of CRC.

3.5. The nucleotide binding domain of GRP78 is responsible for the binding of FMBP

According to the 3D structure of human GRP78[32,33], GRP78 is composed of two domains: one is nucleotide binding domain

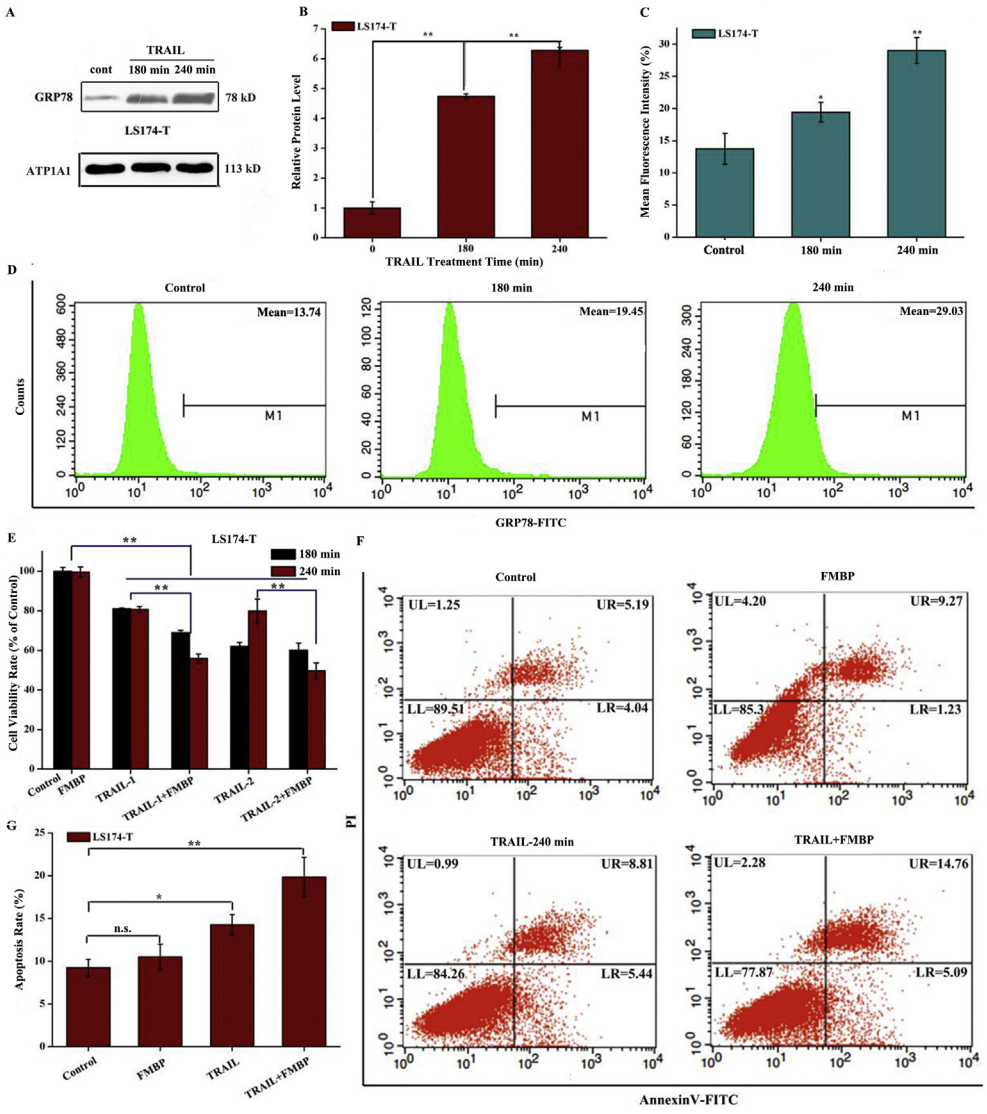

Figure 4 Enhanced csGRP78 induced by TRAIL promotes the anti-CRC sensitivity of FMBP. (A) and (B) Effect of TRAIL treatment on the expression level of csGRP78 in LS174-T cells was measured by Western blot assay. Quantitative analysis was performed by Image J software. (C) and (D) The expression of csGRP78 was analyzed by flow cytometry in LS174-T cells treated with TRAIL for 180 or 240 min. (E) Effect of FMBP treatment on cell growth in LS174-T cells pre-treated with TRAIL for various time intervals. (F) and (G) Pro-apoptotic effect of FMBP was analyzed by flow cytometry in LS174-T cells pre-treated with TRAIL for 240 min. All Data are shown as the mean ± SD ($n = 3$) and analyzed by Student's t-test. *$P < 0.05$, **$P < 0.01$. n.s., not significant.

(NBD) from Val31 to Gly407 capturing and hydrolyzing ATP, and the other is substrate-binding domain (SBD) from Thr423 to Leu654 binding a GRP78-targeting polypeptides, as shown in Fig. 6A. Many studies have demonstrated that the binding of ATP to the NBD of GRP78 induces conformational changes of its SBD, and thus triggers the anti-apoptotic activity of GRP78[34,35]. In this regard, the NBD of GRP78 is necessary for its anti-apoptotic function. Recent study showed that the residues (Asp400 to Asp500) of GRP78 were responsible for translocation of GRP78 from ER to plasma membrane[36]. Hence, to investigate whether FMBP interfered the anti-apoptotic function of GRP78 by binding to the NBD of GRP78, the truncated body of GFP-GRP78-N500 was constructed (Fig. 6A). Subsequently, LS174-T cells were transfected with GFP, GFP-GRP78-N500, respectively. As shown in Fig. 6B and Supporting Information Fig. S4, the results of Western blot and immunofluorescence analysis showed that the N500 truncated body of GRP78 was successfully overexpressed on the membrane surface of LS174-T cells. Interestingly, in LS174-T cells with overexpressed GFP-GRP78-N500, the sensitivity of LS174-T cells to FMBP was markedly increased, characterized by the reduction of the cell survival rate and the increase of cell apoptosis rate (Fig. 6C–E). Similarly, ROS accumulation induced by FMBP was enhanced in LS174-T cells transfected with GFP-GRP78-N500 (Fig. 6F and G). These findings indicate FMBP disturbs the anti-apoptotic activity of csGRP78 to exhibit the anti-CRC effects through directly binding to the NBD of csGRP78.

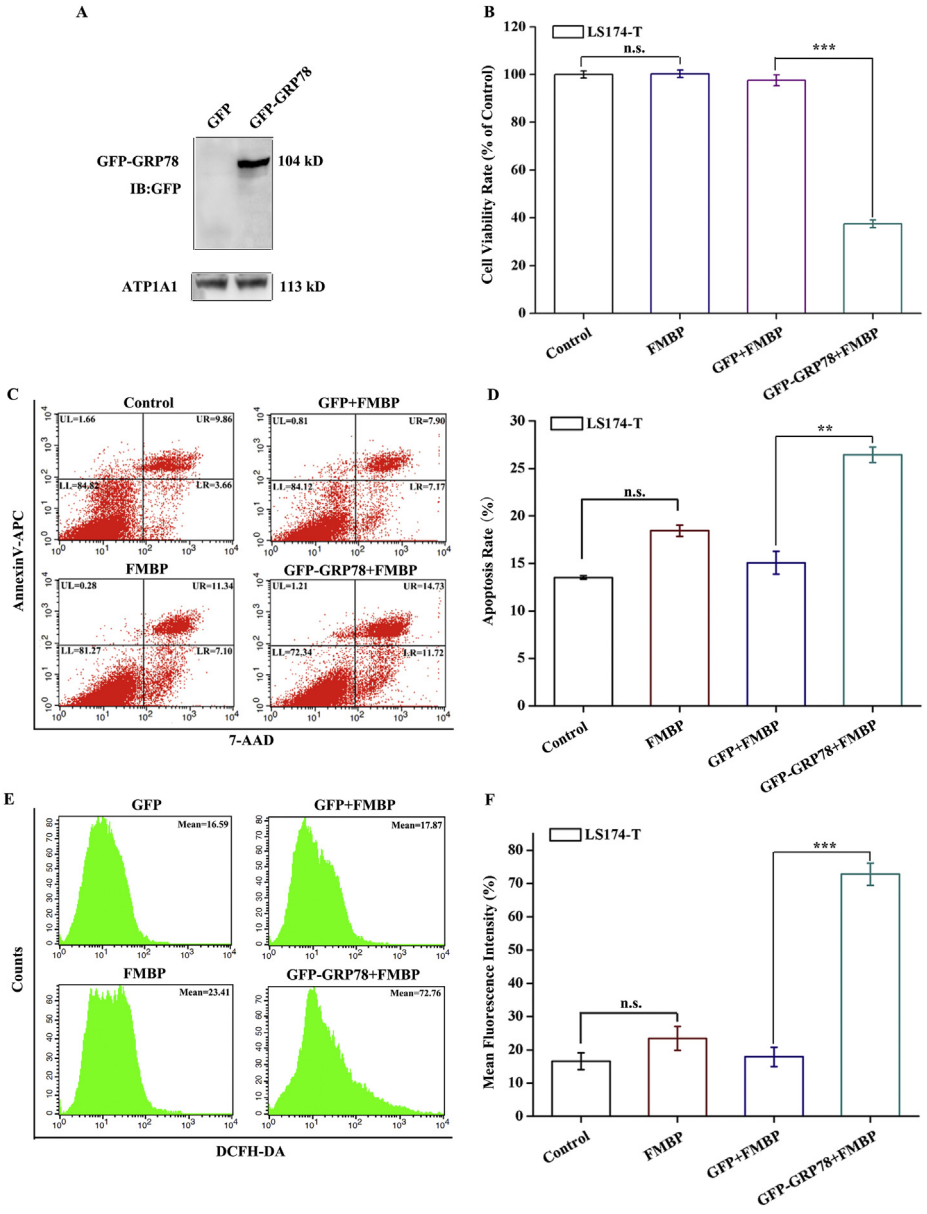

Figure 5 Overexpression csGRP78 promotes the anti-CRC effects of FMBP. (A) The expression of csGRP78 was analyzed in LS174-T cells transfected with GFP or GFP-GRP78 by Western blot assay. (B) Effect of FMBP treatment on cell viability rate in LS174-T cells transfected with GFP or GFP-GRP78 was determined by MTT assay. (C) and (D) The pro-apoptotic effect of FMBP on LS174-T cells transfected with GFP or GFP-GRP78 was analyzed by flow cytometry. (E) and (F) ROS level induced by FMBP in LS174-T cells transfected with GFP or GFP-GRP78 was analyzed by flow cytometry. All data are shown as the mean ± SD ($n = 3$) and analyzed by Student's *t*-test. $^{**}P < 0.01$, $^{***}P < 0.001$ *vs.* GFP + FMBP group. n.s., not significant.

3.6. FMBP induces STAT3 inactivation by combining with csGRP78 of CRC

Potential effects of FMBP on CRC progression by binding to csGRP78 prompted us to explore the downstream effectors of csGRP78. Our previous studies found that FMBP could significantly decrease STAT3 phosphorylation to exhibit anti-CRC activity[20]. Therefore, we speculate that STAT3 may be a downstream signal factor that FMBP exerts anti-CRC activity through binding to csGRP78 (Fig. 7A). Subsequently, co-immunoprecipitation (Co-IP) assay further verified that there is an interaction between csGRP78 and STAT3 in DLD1 cells (Fig. 7B). Interestingly, the inhibitory effect of FMBP on STAT3 phosphorylation was drastically neutralized by blocking GRP78 with anti-GRP78 antibody in DLD1 cells (Fig. 7C and D), indicating the binding of FMBP with csGRP78 may interfere with the phosphorylation of STAT3. To prove this hypothesis, the effects of FMBP on STAT3 and p-STAT3 were measured in LS174-T cells transfected with GFP-GRP78/GFP-GRP78-500. Expectedly, as presented in Fig. 7E and F, overexpressed GRP78/GRP78-500 aggravated the reduction of p-STAT3 and STAT3 levels. Further, the anti-CRC effects induced by FMBP, including the decrease of STAT3, p-STAT3 levels and cell viability radio, the increase of ROS level, was abolished by the activator of STAT3 (Garcinone D) (Fig. 7G–J). Accordingly, these

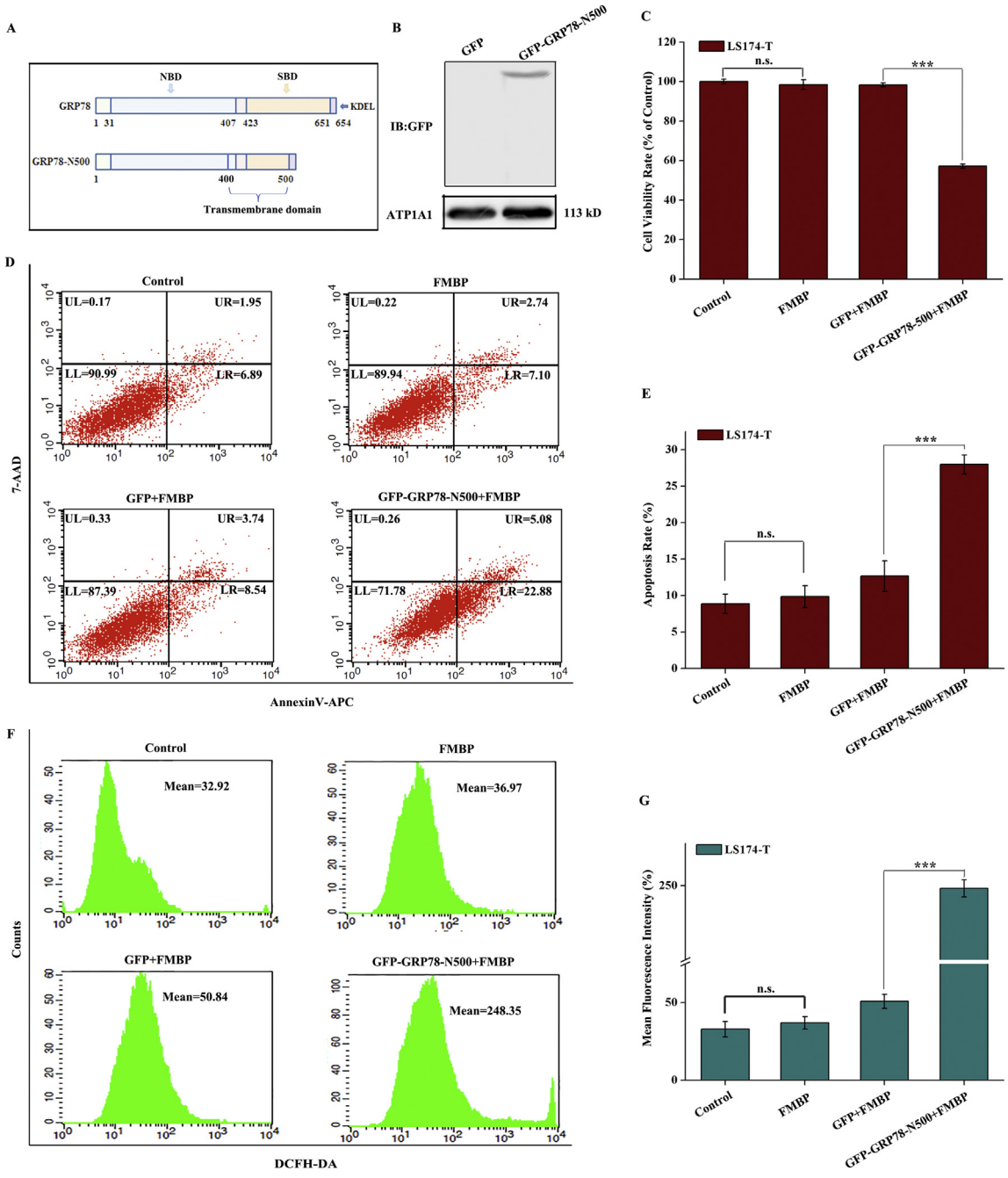

Figure 6 FMBP exerts anti-CRC effect by binding to the NBD of csGRP78. (A) Schematic drawing of human GRP78 functional domains and their amino acid spans. (B) The level of GFP-GRP78-N500 on cell surface in LS174-T cells transfected with GFP-GRP78-N500 was analyzed by Western blot assay. (C) Effect of FMBP treatment on the growth in LS174-T cells transfected with GFP-GRP78-N500 was determined by MTT assay. (D, E) The pro-apoptotic effect of FMBP on LS174-T cells transfected with GFP-GRP78-N500 was analyzed by flow cytometry. (F, G) Effects of FMBP on ROS accumulation in LS174-T cells transfected with GFP-GRP78-N500 was analyzed by flow cytometry. Data are shown as the mean ± SD ($n = 3$) and analyzed by Student's *t*-test. ***$P < 0.001$ compared with GFP + FMBP group. n.s., not significant.

findings indicate the STAT3 is a mediator that FMBP induces the anti-CRC effects through binding to csGRP78.

3.7. csGRP78 is essential for FMBP against CRC growth in xenografted nude mice

To determine csGRP78 plays a key role in the antagonistic effects of FMBP on CRC *in vivo*, the xenografted nude mice model was constructed with LS174-T^{GFP} cells and LS174-T$^{GFP\text{-}GRP78\text{-}N500}$ cells, respectively, followed by intraperitoneal treatment with FMBP (Fig. 8A). The result show that in tumor tissue of mice with highly expressed GFP-GRP78-N500 (Fig. 8B), the tumor volumes and weight in mice showed a significant reduction with FMBP administration, but had little effect on tumor grown with overexpressed GFP (Fig. 8C−F). Next, the expression levels of GRP78, Ki67, p-STAT3 and activated-caspase3 in tumor issue were

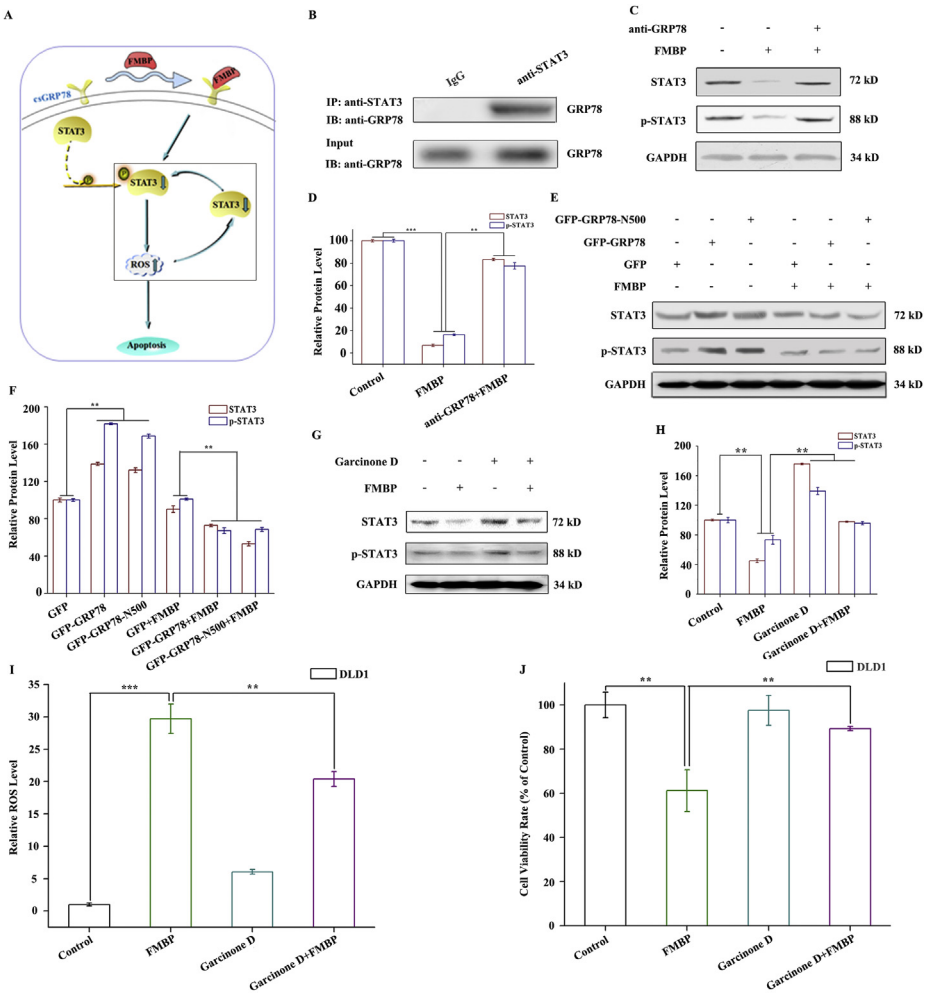

Figure 7 FMBP induces STAT3 inactivation *via* combining with csGRP78 of CRC. (A) Diagram illustrating the molecular target of FMBP against CRC and its signal pathway. (B) The interaction of csGRP78 and STAT3 was determined by coimmunoprecipitation assay. (C, D) Blocking csGRP78 with anti-GRP78 antibody reversed the inhibitory effects of STAT3 and p-STAT3 induced by FMBP in DLD1 cells. Data are shown as the mean ± SD ($n = 3$) and analyzed by Student's *t*-test. $^{**}P < 0.01$, $^{***}P < 0.001$. (E) and (F) Effects of FMBP on levels of STAT3 and p-STAT3 in LS174-T cells overexpressed with GFP-GRP78 or GFP-GRP78-N500. Data are shown as the mean ± SD ($n = 3$) and analyzed by Student's *t*-test. $^{**}P < 0.01$. (G, H) Effects of FMBP on the levels of STAT3 and p-STAT3 in DLD1 cells treated with Garcinone D. Data are shown as the mean ± SD ($n = 3$) and analyzed by Student's *t*-test. $^{**}P < 0.01$. (I) ROS level was measured in DLD1 cells co-treated with 3 μmol/L FMBP and 5 μmol/L Garcinone D. Data are shown as the mean ± SD ($n = 3$) and analyzed by Student's *t*-test. $^{**}P < 0.01$, $^{***}P < 0.001$. (J) Cell viability rate was measured in DLD1 cells co-treated with 3 μmol/L FMBP and 5 μmol/L Garcinone D by MTT assay. Data are shown as the mean ± SD ($n = 3$) and analyzed by Student's *t*-test. $^{**}P < 0.01$.

examined by immunohistochemistry assays. As expected, FMBP significantly reduced the level of p-STAT3 and Ki67 only in tumor tissue of overexpressed GRP78-N500, and increased the level of activated-caspase3 (Fig. 9), which were consistent with the data from the *in vitro* experiments. H&E-stained sections show that FMBP treatment had no effect on the main organs (heart, liver, spleen, lung, kidney and pancreas) of the nude mice (Supporting Information Fig. S5). These results suggest that GRP78 is essential for the targeted anti-CRC effect induced by FMBP *in vivo*.

4. Discussion

Our previous study firstly found that a 35 kDa secretory peroxidase (FMBP) exacted from millet bran displayed prominent anti-CRC activities *in vitro* and in nude mice[19]. Recently, the characteristics and effectiveness of FMBP in clinical application were evaluated by classical colitis-associated carcinogenesis (CAC) mice model which mimicked the inflamed colon and carcinogenesis conditions in humans. As expected, FMBP significantly restrained the growth of colonic neoplasms in CAC mice model, and effectively recovered intestinal length and body weight, prolonged the survival rate of CAC mice[21], fully indicating that FMBP has potential clinical application in the treatment of CRC. Interestingly, in these previous studies, we observed that FMBP had little effect on the growth of normal colonic epithelial cells and mice while inhibiting CRC tumor, suggesting that it has a good specificity for CRC. Therefore, it is very important to identify the specific molecular target of FMBP against CRC, contributing to develop it as a promising targeted drug for CRC in the future.

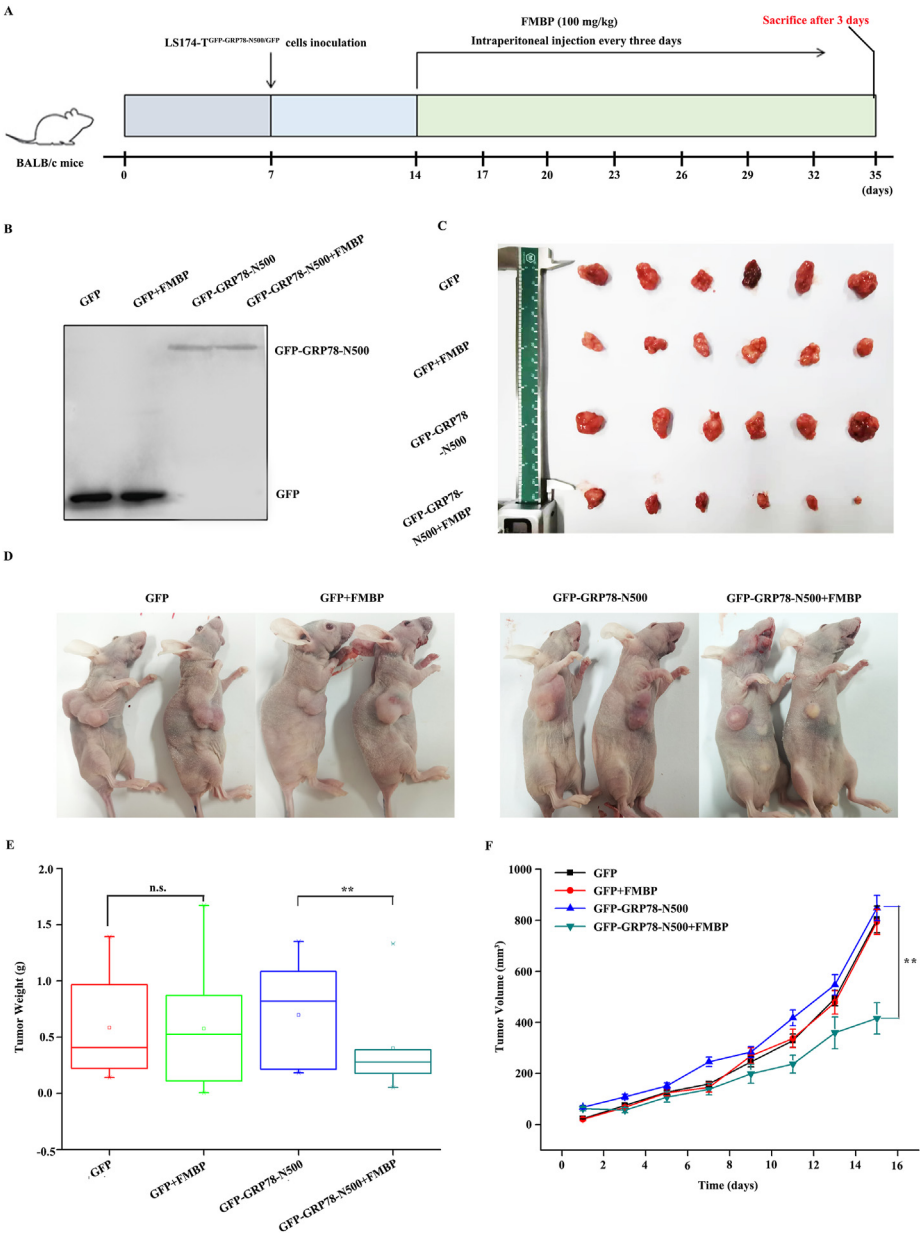

Figure 8 csGRP78 is essential for FMBP against CRC growth in xenografted nude mice. (A) Establishment of xenografted nude mice model with stably overexpressed GFP or GFP-GRP78-N500 of LS174-T cells. (B) The expression level of GFP-GRP78-N500 in tumor tissues was analyzed by Western blot assay. (C) Representative tumor samples were exhibited in different groups ($n = 6$). (D) Representative images of mice at the sacrifice in the GFP, GFP + FMBP, GFP-GRP78-N500 and GFP-GRP78-N500+FMBP groups. Mice were sacrificed on the 35th day and tumors were excised ($n = 6$). (E) Tumor weight was calculated in each group ($n = 6$); $^{**}P < 0.01$ *vs*. GFP-GRP78-N500 group. (F) Tumor volume of different groups ($n = 6$); $^{**}P < 0.01$ compared with GFP-GRP78-N500 group. Data are shown as the mean ± SD and analyzed by Student's *t*-test. $^{**}P < 0.01$. n.s., not significant.

Our present results found that FMBP did not enter the cells, but located on the cell membrane (Fig. S1), speculating that FMBP may exert a targeted effect on CRC through interacting with the receptor on the surface of CRC cells. Many studies have shown that cell surface receptors overexpressed in cancer cells, and especially those expressed only on tumor cells but not on normal cells, play important roles in cancer targeted therapy and diagnosis[37,38]. Hence, Bio-FMBP was used to pull down the cell surface target of FMBP. Subsequent MALDI TOF/TOF analysis and CETSA assay results show that csGRP78 located on the surface of CRC was a specific interaction protein with FMBP (Fig. 1). Encouragingly, csGRP78 frequently located abnormally on the surface of many tumor cells (colon cancer, prostate, and breast cancer, etc.), but not in normal cell surface, which can promote tumor progress[10,39,40], and open up an exciting opportunity of tumor specific targeting function[33]. Hence, csGRP78 becomes a promising cancer cell-specific biomarker and an attractive therapeutic target for cancer. Emerging evidence has shown that some molecules, such as human IgM monoclonal antibody PAT-SM6 and isthmin (ISM), can bind to csGRP78 to activate the apoptotic pathways as attractive novel agents against cancer[31,41]. Our present results found that the anti-CRC sensitivity

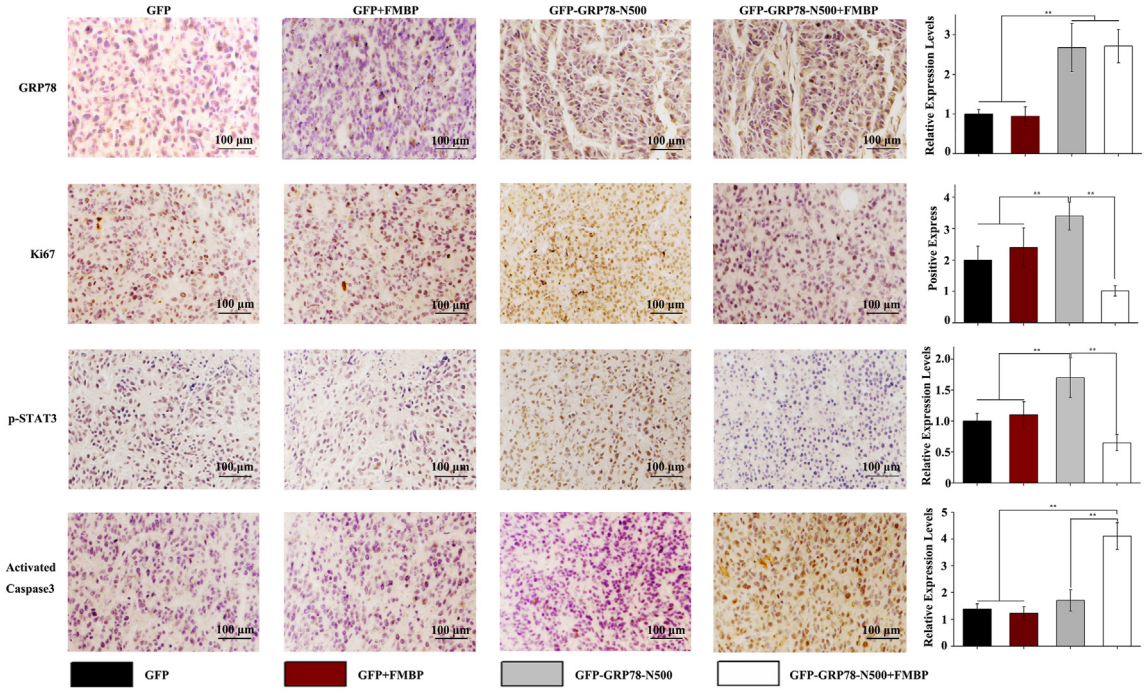

Figure 9 The expression levels of GRP78, p-STAT3, Ki67 and actived-caspase3 in tumor tissues were analyzed by IHC staining. Quantitative analysis was carried out by image J software. Scale bar: 100 μm. Data are shown as the mean ± SD ($n = 6$); $^{**}P < 0.01$.

of FMBP was positively correlated with the expression levels of csGRP78 in CRC (Figs. 2 and 8). Specifically, blocking csGRP78 attenuated the anti-CRC effects induced by FMBP, including cell viability and colony formation ability, the levels of cell apoptosis and ROS production (Fig. 3), while the overexpression of csGRP78 showed an opposite trend (Figs. 4 and 5), suggesting csGRP78 is the specific target of FMBP against CRC.

Previous studies have revealed that specifically intervening the ATPase function of GRP78 could effectively inactivate GRP78 in cancer. Hence, the ATPase catalytic activity was necessary for the anti-apoptotic function of GRP78 through preventing caspase activation[42]. For example, some compounds, such as EGCG, honokiol and aspirin, increase the chemotoxic sensibility toward cancer cells by directly binding to GRP78-NBD to inhibit the ATPase activity[43−45]. Excitedly, in our current study, the subsequent anti-tumor activity assay demonstrated that in CRC LS174-T cells, overexpressed GRP78-N500 truncation (including NBD and membrane translocation sequences) could significantly increase the chemotoxic sensitivity of FMBP to LS174-T cells, accompanied by the elevation of ROS production and the apoptosis rate, as well as the reduction of cell viability radio (Fig. 6), which implies that FMBP combines to the NBD domain of csGRP78 to exhibit anti-CRC effects. As a receptor on the surface of tumor cells, csGRP78 can interact with a variety of signaling molecules to trigger STAT3, RAS/MAPK and PI3-kinase/AKT/mTOR downstream signaling cascades, promoting cellular proliferation and survival[33,46]. Binding of ATP to the NBD of GRP78 allosterically accelerates polypeptide binding and release *via* inducing conformational changes of SBD[34]. Therefore, we speculate that the binding of csGRP78-NBD to FMBP may interfere with its anti-apoptotic function by restraining the ATPase activity, blocking the downstream signaling pathways associated with apoptosis, thus leading to apoptosis of CRC cells.

STAT3 plays a vital role in cell survival and tumorigenesis[47]. Our previous study found that FMBP induced the accumulation of intracellular ROS to inhibit the activation of STAT3, leading to the inhibition of CRC cell proliferation[20,22]. Interestingly, GRP78 was highly expressed in tumors, accompanied by the elevated STAT3 phosphorylation, and the STAT3 signaling pathway activated by GRP78, a well-known signaling pathway involved in the progression of multiple tumors, such as breast cancer, cervical cancer and colon cancer[20,48,49]. Consistently, our present results also showed that the expression of csGRP78 was positively correlated with the expression of p-STAT3 and STAT3 in CRC cells (Fig. 7). Intriguingly, blocking csGRP78 drastically neutralized the inhibitory effect of FMBP on p-STAT3 and STAT3 in DLD1 cells, while which exhibited a contrary tendency in LS174-T cells overexpressed with GFP-GRP78 or GFP-GRP78-N500 (Fig. 7C−F). Therefore, we speculate that STAT3, as a downstream effector of csGRP78, may be involved in the anti-CRC effect of FMBP. Further, we found that an anti-STAT3 antibody presented cross-immunoprecipitation with csGRP78 (Fig. 7B), which means that there is an interaction between csGRP78 and STAT3 in CRC cells. This is inconsistent with the previous study showing that STAT3 was not associated with GRP78 in breast cancer[50], indicating that the activation pathway of STAT3 induced by csGRP78 may be different in different cancer cells. Considering that STAT3 is located in the cytoplasm[51], csGRP78 has no classical transmembrane domain[52]; rather preferentially exists as a peripheral protein binding to other cell surface proteins on the plasma membrane of stressed cancer cells. We speculate that csGRP78 may activate STAT3 phosphorylation by recruiting STAT3 and other transmembrane proteins to form a complex in CRC cells, which can be interfered by FMBP, thus results in the inactivation of STAT3. More studies are needed to further define this possibility. There is evidence showing that STAT3 and ROS in

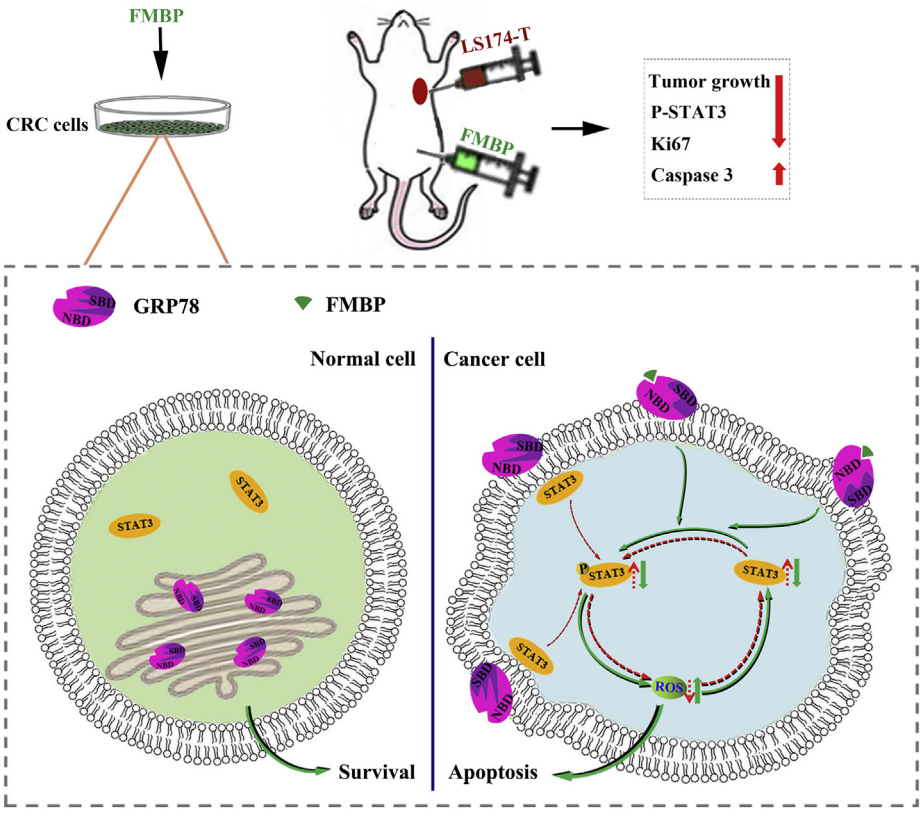

Figure 10 Diagram illustrating the molecular mechanism of FMBP against CRC. csGRP78 is often abnormally expressed on cell surface of CRC. FMBP restrains the activation of STAT3 through directly binding to the NBD of csGRP78 on CRC cell surface, and promotes the excessive accumulation of downstream ROS, resulting in blockage of CRC development. Fortunately, due to almost no expression of csGRP78 on the surface of normal colon epithelial cells, and thus, FMBP had no effect on the growth of normal cells. Consistently, these phenomena have been confirmed *in vivo*. Hence, csGRP78 serves as an underlying target for FMBP against CRC.

tumor cells are regulated by each other, which forms a cycle to maintain the homeostasis of tumor cells[53,54]. In this regard, we speculate that the accumulation of ROS induced by FMBP is realized by the binding to csGRP78 to inactivate STAT3. As expected, the deduction was confirmed with the activator of STAT3 (Garcinone D). As shown in Fig. 7I, compared to only FMBP treatment, Garcinone D and FMBP co-treatment dramatically reduced the ROS accumulation and cell viability rate in CRC cells. Hence, these results indicate STAT3 is the mediator of ROS elevation induced by FMBP *via* csGRP78.

5. Conclusions

Our research demonstrated that csGRP78, which abnormally expresses on CRC cell surface but not on normal cell surface, is an underlying target for FMBP to exert specific anti-CRC effect *in vitro* and *in vivo*. Specifically, in CRC cells, FMBP restrains the activation of STAT3 signal pathway through directly binding to the NBD of csGRP78, and promotes the excessive accumulation of downstream ROS, resulting in blocking the development of CRC. Fortunately, due to almost no expression of csGRP78 on the surface of normal colon cells, and thus, FMBP had no effect on the growth of normal cells. Consistently, these phenomena have been confirmed *in vivo* (Fig. 10). Collectively, our data will hopefully support FMBP has the potential to be developed as a targeted drug for the treatment of CRC in the future.

Acknowledgments

This study was supported by National Natural Science Foundation of China (Nos. 31500630, 31770382, 32072220, and 81803238); "1331 Project" Key Innovation Center and Team, National Key Research and Development Project (No. 2020YFD1001405, China); Shanxi Key Laboratory for Research and Development of Regional Plants, Higher Education Institution Project of Shanxi Province: Ecological Remediation of Soil Pollution Disciplines Group (No. 20181401, China); the Open Project Program of Xinghuacun College of Shanxi University [Shanxi Institute of Brewing Technology and Industry (Preparation)] (No. XCSXU-KF-202004, China).

Author contributions

Zhuoyu Li and Shuhua Shan participated in the research design and guidance. Shuhua Shan and Jinping Niu performed the experiments, analysed the data and wrote the manuscript. Ruopeng Yin, Jiangying Shi, Lizhen, Zhang and Caihong, Wu assisted with establishment of nude tumor model. Hanqing Li assisted with the data analysis. Zhuoyu, Li modified the manuscript.

Conflicts of interest

The authors have declared no conflicts of interest.

Appendix A. Supporting information

Supporting data to this article can be found online at https://doi.org/10.1016/j.apsb.2021.10.004.

References

1. Bray F, Ferlay J, Soerjomataram I, Siegel RL, Torre LA, Jemal A. Global cancer statistics 2018: GLOBOCAN estimates of incidence and mortality worldwide for 36 cancers in 185 countries. *CA Cancer J Clin* 2018;**68**:394−424.
2. Wei QY, Xu YM, Lau ATY. Recent progress of nanocarrier-based therapy for solid malignancies. *Cancers* 2020;**12**:2783.
3. Lee YT, Tan YJ, Oon CE. Molecular targeted therapy: treating cancer with specificity. *Eur J Pharmacol* 2018;**834**:188−96.
4. Ingham M, Schwartz GK. Cell-cycle therapeutics come of age. *J Clin Oncol* 2017;**35**:2949−59.
5. Reddy PS, Lokhande KB, Nagar S, Reddy VD, Murthy PS, Swamy KV. Molecular modeling, docking, dynamics and simulation of gefitinib and its derivatives with EGFR in non-small cell lung cancer. *Curr Comput Aided Drug Des* 2018;**14**:246−52.
6. Augustine T, Maitra R, Zhang J, Nayak J, Goel S. Sensitization of colorectal cancer to irinotecan therapy by PARP inhibitor rucaparib. *Invest N Drugs* 2019;**37**:948−60.
7. Guo L, Zhang H, Chen B. Nivolumab as programmed death-1 (PD-1) inhibitor for targeted immunotherapy in tumor. *J Cancer* 2017;**8**:410−6.
8. Ni M, Zhang Y, Lee AS. Beyond the endoplasmic reticulum: atypical GRP78 in cell viability, signalling and therapeutic targeting. *Biochem J* 2011;**434**:181−8.
9. Lee AS. Glucose-regulated proteins in cancer: molecular mechanisms and therapeutic potential. *Nat Rev Cancer* 2014;**14**:263−76.
10. Li Z, Zhang L, Zhao Y, Li H, Xiao H, Fu R, et al. Cell-surface GRP78 facilitates colorectal cancer cell migration and invasion. *Int J Biochem Cell Biol* 2013;**45**:987−94.
11. Gonzalez-Gronow M, Pizzo SV, Misra UK. GRP78 (BiP): a multifunctional cell surface receptor. In: Henderson B, Pockley A, editors. *Cellular trafficking of cell stress proteins in health and disease*. Dordrecht: Springer Netherlands; 2012. p. 229−42.
12. Arap MA, Lahdenranta J, Mintz PJ, Hajitou A, Sarkis AS, Arap W, et al. Cell surface expression of the stress response chaperone GRP78 enables tumor targeting by circulating ligands. *Cancer Cell* 2004;**6**:275−84.
13. Liu R, Li X, Gao W, Zhou Y, Wey S, Mitra SK, et al. Monoclonal antibody against cell surface GRP78 as a novel agent in suppressing PI3K/AKT signaling, tumor growth, and metastasis. *Clin Cancer Res* 2013;**19**:6802−11.
14. McFarland BC, Stewart Jr J, Hamza A, Nordal R, Davidson DJ, Henkin J, et al. Plasminogen kringle 5 induces apoptosis of brain microvessel endothelial cells: sensitization by radiation and requirement for GRP78 and LRP1. *Cancer Res* 2009;**69**:5537−45.
15. Burikhanov R, Zhao Y, Goswami A, Qiu S, Rangnekar VM. The tumor suppressor Par-4 activates an extrinsic pathway for apoptosis. *Cell* 2009;**138**:377−88.
16. Zhang L, Li Z, Shi T, La X, Li H, Li Z. Design, purification and assessment of GRP78 binding peptide-linked subunit A of subtilase cytotoxic for targeting cancer cells. *BMC Biotechnol* 2016;**16**:65.
17. Wang Y, Wu H, Li Z, Yang P, Li Z. A positive feedback loop between GRP78 and VPS34 is critical for GRP78-mediated autophagy in cancer cells. *Exp Cell Res* 2017;**351**:24−35.
18. Li Z, Zhao C, Li Z, Zhao Y, Shan S, Shi T, et al. Reconstructed mung bean trypsin inhibitor targeting cell surface GRP78 induces apoptosis and inhibits tumor growth in colorectal cancer. *Int J Biochem Cell Biol* 2014;**47**:68−75.
19. Shan S, Li Z, Newton IP, Zhao C, Li Z, Guo M. A novel protein extracted from foxtail millet bran displays anti-carcinogenic effects in human colon cancer cells. *Toxicol Lett* 2014;**227**:129−38.
20. Shan S, Li Z, Guo S, Li Z, Shi T, Shi J. A millet bran-derived peroxidase inhibits cell migration by antagonizing STAT3-mediated epithelial-mesenchymal transition in human colon cancer. *J Funct Foods* 2014;**10**:444−55.
21. Shan S, Wu C, Shi J, Zhang X, Niu J, Li H, et al. Inhibitory effects of peroxidase from Foxtail Millet Bran on colitis-associated colorectal carcinogenesis by the blockade of glycerophospholipid metabolism. *J Agric Food Chem* 2020;**68**:8295−307.
22. Shan S, Shi J, Li Z, Gao H, Shi T, Li Z, et al. Targeted anti-colon cancer activities of a millet bran-derived peroxidase were mediated by elevated ROS generation. *Food Funct* 2015;**6**:2331−8.
23. La X, Zhang L, Li H, Li Z, Song G, Yang P, et al. Ajuba receptor mediates the internalization of tumor-secreted GRP78 into macrophages through different endocytosis pathways. *Oncotarget* 2018;**9**:15464−79.
24. Martinez Molina D, Jafari R, Ignatushchenko M, Seki T, Larsson EA, Dan C, et al. Monitoring drug target engagement in cells and tissues using the cellular thermal shift assay. *Science* 2013;**341**:84−7.
25. Notaro A, Sabella S, Pellerito O, Di Fiore R, De Blasio A, Vento R, et al. Involvement of PAR-4 in cannabinoid-dependent sensitization of osteosarcoma cells to TRAIL-induced apoptosis. *Int J Biol Sci* 2014;**10**:466−78.
26. Devitt G, Thomas M, Klibanov AM, Pfeiffer T, Bosch V. Optimized protocol for the large scale production of HIV pseudovirions by transient transfection of HEK293T cells with linear fully deacylated polyethylenimine. *J Virol Methods* 2007;**146**:298−304.
27. Zhang L, Li Z, Ding G, La X, Yang P, Li Z. GRP78 plays an integral role in tumor cell inflammation-related migration induced by M2 macrophages. *Cell Signal* 2017;**37**:136−48.
28. Kang JM, Park S, Kim SJ, Hong HY, Jeong J, Kim HS, et al. CBL enhances breast tumor formation by inhibiting tumor suppressive activity of TGF-β signaling. *Oncogene* 2012;**31**:5123−31.
29. Chang J, Kim Y, Kwon HJ. Advances in identification and validation of protein targets of natural products without chemical modification. *Nat Prod Rep* 2016;**33**:719−30.
30. Jafari R, Almqvist H, Axelsson H, Ignatushchenko M, Lundbäck T, Nordlund P, et al. The cellular thermal shift assay for evaluating drug target interactions in cells. *Nat Protoc* 2014;**9**:2100−22.
31. Chen M, Zhang Y, Yu VC, Chong YS, Yoshioka T, Ge R. Isthmin targets cell-surface GRP78 and triggers apoptosis *via* induction of mitochondrial dysfunction. *Cell Death Differ* 2014;**21**:797−810.
32. Wang SH, Lee AC, Chen IJ, Chang NC, Wu HC, Yu HM, et al. Structure-based optimization of GRP78-binding peptides that enhances efficacy in cancer imaging and therapy. *Biomaterials* 2016;**94**:31−44.
33. Farshbaf M, Khosroushahi AY, Mojarad-Jabali S, Zarebkohan A, Valizadeh H, Walker PR. Cell surface GRP78: an emerging imaging marker and therapeutic target for cancer. *J Control Release* 2020;**328**:932−41.
34. Bailly C, Waring MJ. Pharmacological effectors of GRP78 chaperone in cancers. *Biochem Pharmacol* 2019;**163**:269−78.
35. Nicolaï A, Delarue P, Senet P. Decipher the mechanisms of protein conformational changes induced by nucleotide binding through free-energy landscape analysis: ATP binding to Hsp70. *PLoS Comput Biol* 2013;**9**:e1003379.
36. Tsai YL, Zhang Y, Tseng CC, Stanciauskas R, Pinaud F, Lee AS. Characterization and mechanism of stress-induced translocation of 78-kilodalton glucose-regulated protein (GRP78) to the cell surface. *J Biol Chem* 2015;**290**:8049−64.
37. Tashima T. Effective cancer therapy based on selective drug delivery into cells across their membrane using receptor-mediated endocytosis. *Bioorg Med Chem Lett* 2018;**28**:3015−24.
38. Guo M, Zhang H, Zheng J, Liu Y. Glypican-3: a new target for diagnosis and treatment of hepatocellular carcinoma. *J Cancer* 2020;**11**:2008−21.
39. Lee AS. GRP78 induction in cancer: therapeutic and prognostic implications. *Cancer Res* 2007;**67**:3496−9.

40. Ge R, Kao C. Cell surface GRP78 as a death receptor and an anti-cancer drug target. *Cancers* 2019;**11**:1787.
41. Rasche L, Duell J, Morgner C, Chatterjee M, Hensel F, Rosenwald A, et al. The natural human IgM antibody PAT-SM6 induces apoptosis in primary human multiple myeloma cells by targeting heat shock protein GRP78. *PLoS One* 2013;**8**:e63414.
42. Reddy RK, Mao C, Baumeister P, Austin RC, Kaufman RJ, Lee AS. Endoplasmic reticulum chaperone protein GRP78 protects cells from apoptosis induced by topoisomerase inhibitors: role of ATP binding site in suppression of caspase-7 activation. *J Biol Chem* 2003;**278**:20915−24.
43. Ermakova SP, Kang BS, Choi BY, Choi HS, Schuster TF, Ma WY, et al. (−)-Epigallocatechin gallate overcomes resistance to etoposide-induced cell death by targeting the molecular chaperone glucose-regulated protein 78. *Cancer Res* 2006;**66**:9260−9.
44. Martin S, Lamb HK, Brady C, Lefkove B, Bonner MY, Thompson P, et al. Inducing apoptosis of cancer cells using small-molecule plant compounds that bind to GRP78. *Br J Cancer* 2013;**109**:433−43.
45. Zhang X, Chen J, Cheng C, Li P, Cai F, Xu H, et al. Aspirin potentiates celecoxib-induced growth inhibition and apoptosis in human non-small cell lung cancer by targeting GRP78 activity. *Ther Adv Med Oncol* 2020;**12**:1758835920947976.
46. Tseng CC, Zhang P, Lee AS. The COOH-terminal proline-rich region of GRP78 is a key regulator of its cell surface expression and viability of tamoxifen-resistant breast cancer cells. *Neoplasia* 2019;**21**:837−48.
47. Siveen KS, Sikka S, Surana R, Dai X, Zhang J, Kumar AP, et al. Targeting the STAT3 signaling pathway in cancer: role of synthetic and natural inhibitors. *Biochim Biophys Acta* 2014;**1845**:136−54.
48. Ma JH, Qin L, Li X. Role of STAT3 signaling pathway in breast cancer. *Cell Commun Signal* 2020;**18**:33.
49. Ramírez de Arellano A, Lopez-Pulido EI, Martínez-Neri PA, Estrada Chávez C, González Lucano R, Fafutis-Morris M, et al. STAT3 activation is required for the antiapoptotic effects of prolactin in cervical cancer cells. *Cancer Cell Int* 2015;**15**:83.
50. Yao X, Liu H, Zhang X, Zhang L, Li X, Wang C, et al. Cell surface GRP78 accelerated breast cancer cell proliferation and migration by activating STAT3. *PLoS One* 2015;**10**:e0125634.
51. Lee H, Jeong AJ, Ye SK. Highlighted STAT3 as a potential drug target for cancer therapy. *BMB Rep* 2019;**52**:415−23.
52. Tsai YL, Zhang Y, Tseng CC, Stanciauskas R, Pinaud F, Lee AS. Characterization and mechanism of stress-induced translocation of 78-kilodalton glucose-regulated protein (GRP78) to the cell surface. *J Biol Chem* 2015;**290**:8049−64.
53. Lu L, Dong J, Wang L, Xia Q, Zhang D, Kim H, et al. Activation of STAT3 and Bcl-2 and reduction of reactive oxygen species (ROS) promote radioresistance in breast cancer and overcome of radioresistance with niclosamide. *Oncogene* 2018;**37**:5292−304.
54. Kasiappan R, Jutooru I, Karki K, Hedrick E, Safe S. Benzyl isothiocyanate (BITC) induces reactive oxygen species-dependent repression of STAT3 protein by down-regulation of specificity proteins in pancreatic cancer. *J Biol Chem* 2016;**291**:27122−33.